

## Optical and Electrical Properties of *n*-type Porous Silicon Produced by Electrochemical Etching and Study the Influence of $\gamma$ -irradiation

A.A. Sulaiman<sup>1</sup>, A.A.K. Muhammed<sup>2</sup>, M.M. Ivashchenko<sup>3</sup>

<sup>1</sup> Department of Physics, College of Science, University of Mosul, Mosul, Iraq

<sup>2</sup> Sumy State University, 2, Rimsky-Korsakov St., 40007 Sumy, Ukraine

<sup>3</sup> Konotop Institute of Sumy State University, 24, Myru Ave., 41615 Konotop, Ukraine

(Received 13 May 2019; revised manuscript received 23 October 2019; published online 25 October 2019)

Porous silicon layers were prepared by electrochemical etching. We study the physical and structural properties of porous silicon. Scanning electron microscopy (SEM) and cross sectional SEM have been used to study the effect of  $\gamma$ -irradiation on the pore size of P*Si* for various irradiation doses. The growth in pore width can be attributed to an increasing holes number on the Si surface with increasing  $\gamma$  irradiation dose. The cross-section of the P*Si* layer shows micrographs of the morphology of the P*Si* layer perpendicular to the Si surface, with side branches in the  $\langle 111 \rangle$  orientation. The transmittance spectra of the P*Si* were obtained in the range 320-1200 nm with increasing  $\gamma$  irradiation at 100 Gy, the transmittance of the P*Si* is decreased and the reflectance of P*Si* shows the largest reflectance with increasing irradiation. The analysis of photoluminescence spectra has been shown that the formation of fully penetrated porous silicon can lead to a decrease of the photoluminescence intensity with increasing of  $\gamma$  irradiation dose. It may be caused by the increase of the specific surface area and by the bigger band gap value of P*Si* than for bulk Si. Electrical measurements such as resistivity, conductivity, barrier height, and ideality factor were investigated. The barrier height has small value and the decrease in the barrier height is due to the interface between P*Si* layer and Si wafer which acts as a defect in the interface and also due to the saturation current has maximum value at 100 Gy dose. The ideality factor increased from 1.544 to 17.563 at dose 100 Gy. The resistivity of the porous silicon was  $10^5$ - $10^4$   $\Omega$ .cm which decreased as the irradiation dose of  $\gamma$ -ray increased. The photocurrent spectrum in the range 1.25-3.00 eV shows porous silicon irradiated at dose 100 Gy which contains two peaks at 2.13 and 2.77 eV which lie in the visible region.

**Keywords:** Porous silicon, Irradiation, Electrochemical etching.

DOI: [10.21272/jnep.11\(5\).05025](https://doi.org/10.21272/jnep.11(5).05025)

PACS numbers: 68.55.ag, 72.10.Bg

### 1. INTRODUCTION

Porous silicon (P*Si*) is a structure with a strong absorptivity and with the optical properties in the visible range at room temperature [1]. P*Si* has become interesting in the applications because of the low power consumption and low cost [2]. P*Si* layers were used in the humidity sensors [4] and gas detectors [3]. Several investigations show that the optical and the electrical characteristics of P*Si* semiconductors can be changed in their surfaces [5]. Attractive technique used for fabrication of uniform pores on the Si surface is called electrochemical anodization method [6]. Several parameters are used to study the surface characteristics of P*Si* layer such as etching time, current density, shape of current and electrolyte and light with different frequencies. P*Si* is consisted of constant current electrochemical anodization of Si in HF electrolyte [7].

In the present work, porous silicon has been prepared by electrochemical etching and then we demonstrated the effect of  $\gamma$ -irradiation on the optical, electrical and structural properties of porous silicon.

### 2. EXPERIMENTAL DETAILS

P*Si* was synthesized by using *n*-type Si wafer (111), which was rinsed by using ethanol and acetone to remove oil and dirt. We used (1:10) HF:H<sub>2</sub>O to remove the native oxide layer. Chemical etching procedure allows to prepare porous silicon with usage the electrolyte based on 25 % HF and HNO<sub>3</sub> (1:3) acids. Then the samples were rinsed in ethanol and dried with a jet of nitrogen

gas and stored in a container filled with methanol to avoid the formation of an oxide layer on the porous layer. P*Si* layer was made by anodizing of Si layer in HF at room temperature for 30 mA and period of about 20 min. The solution has hydrofluoric acid (HF 25 %), hydrogen peroxide (H<sub>2</sub>O<sub>2</sub>) and ethanol (95 %) added to the solution to increase the ability of the P*Si* surface. In addition, there is hydrogen evolution in the reaction.

The Si layer serves as the anode and it is sandwiched between the bottom and the top parts of the Teflon which has a circular window of area (1 cm<sup>2</sup>) and it exposes the Si to HF electrolyte and forms the P*Si* layer. The cathode is a circular gold that is covered in the HF electrolyte, it is placed between the top part of an aluminum ring and the Teflon.

Cs-201 radioisotope emitting 662 keV source with a dose rate of 6 Gy/min was used for exposing the samples to various irradiation doses of 50 and 100 Gy at room temperature. The  $\gamma$ -ray source was contained in a JL Shepherd Model 91-12A Irradiator.

Surface morphology of the films was studied by Nanoscope E-2138k Molecular Imaging system scanning electron microscope.

The transmission and reflection spectra were measured in the range of 300-1200 nm by using a CNDB AQ-4315 spectrophotometer.

The *I-V* characteristics were measured at room temperature with a Keithley (3400) source Meter and WX5140s Wacom simulator. For current-voltage measurements, tektronics (CD) multimeter, digital multimeter and a dual farnel LT 30/2 power supply were used. Al was used as a contact layer for n-P*Si* surface.

By using an electron energy analyzer which operated in constant pass energy mode under ultrahigh vacuum (11-10 mbar), we measured the kinetic energy of the photoemitted electrons from the surface.

### 3. RESULTS AND DISCUSSION

#### 3.1 Surface Morphology Study

The surface morphology investigations of the porous layer structure produced by different methods were carried out to estimate the surface area of the porous layer. One of these methods was scanning electron microscopy (SEM). Fig. 1 shows the surface morphology image of samples a, b and c which represent  $\gamma$  irradiation of 0, 50, 100 Gy.

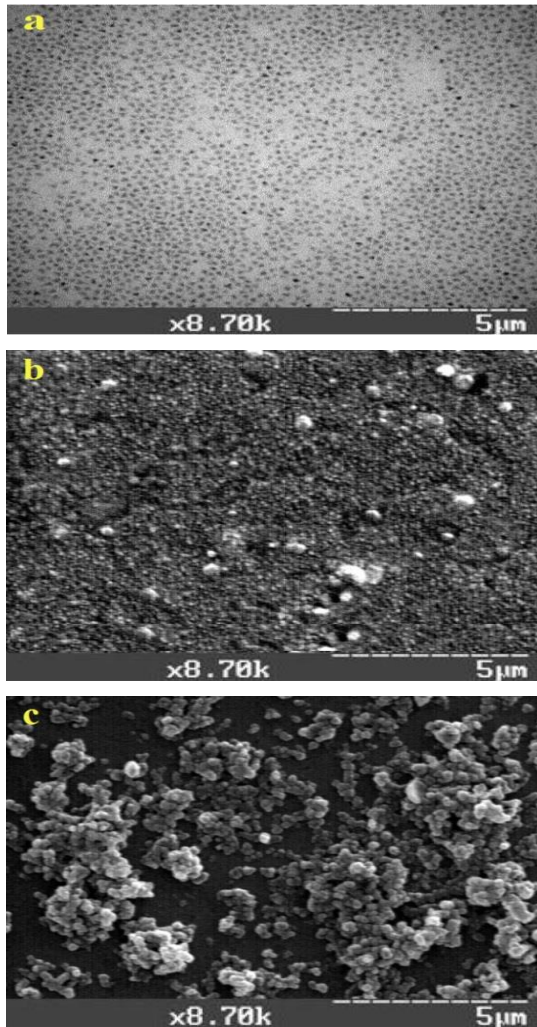


**Fig. 1** – SEM graphs of PSi: without irradiation (a), irradiated at 50 Gy (b) and 100 Gy (c)

Increasing irradiation will form PSi of different pores with trenches size and shapes. These trenches are distributed in the random direction and the pores widths increase with increasing  $\gamma$  irradiation. This layer has pores and trenches with various sizes and shapes in micro- and nanosilicon regions. Large scale trenches do not appear with samples without irradiation but the size of layer pores is very small. Fig. 1 illustrates the morphological characteristics at  $\gamma$  irradiation of 50 and

100 Gy, where a pore-like structure with arrays of small number of large pores close to spherical shape is. This growth in pore width can be attributed to an increasing holes number on the Si surface with increasing  $\gamma$  irradiation dose leading to a preferential dissolution of the nearest-neighbor's pores which promotes the pore-pore overlap [8]. However, the irradiation rates may be different and this could lead to a non-uniformity in the values of the pores width.

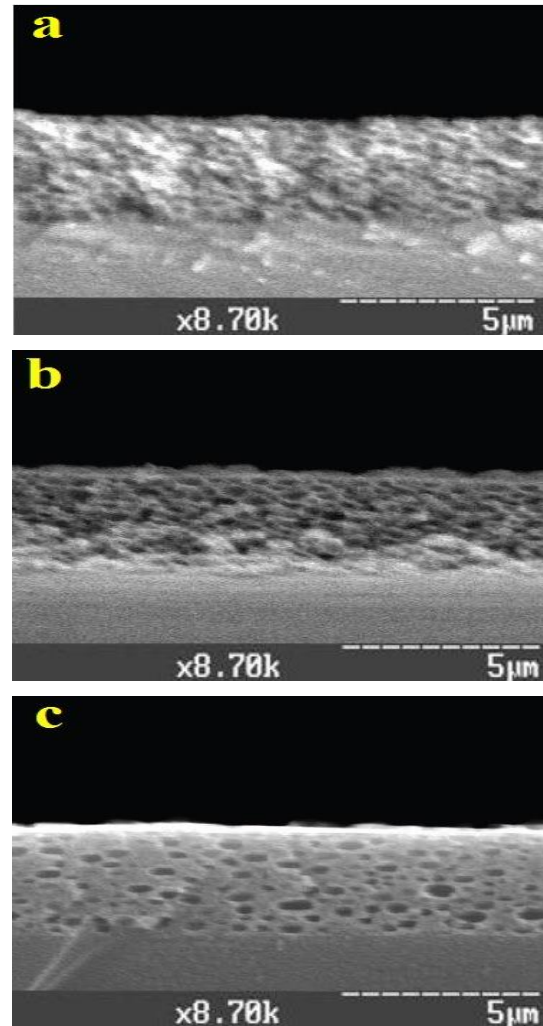


**Fig. 2** – Cross-sectional SEM images of PSi: without irradiation (a), irradiated at 50 Gy (b) and 100 Gy (c)

Based on the SEM micrographs, the cross-section of the PSi layer can be deviled into three distinct figures (a, b and c). Fig. 2 shows micrographs of the morphology of the PSi layer perpendicular to the Si surface with side branches in the  $\langle 111 \rangle$  orientation as depicted in Fig. 1a. This result is in agreement with that observed in [9]. The formation of pores in the  $\langle 111 \rangle$  orientation creates side branches from the main pore. This was due to the availability of many holes and the dissolution came to a halt once the holes depleted in that orientation and this led to the high energy barrier created by the inter-pore distance which became smaller with the progress of dissolution [10]. This pore growth feature persisted upon increasing  $\gamma$  irradiation to 50 Gy, as shown in Fig. 2b. As  $\gamma$  irradiation further increased to

100 Gy, the walls were smoothed and the pores were enlarged, a behavior became more obvious at 100 Gy, as depicted in Fig. 2c. The increment in pore diameter in this case was due to the active dissolution of silicon at the pore wall by increasing amount of  $\gamma$  irradiation which enlarged the pore size and consequently reduced the inter-pore distance.

### 3.2 Optical Properties

The transmittance spectra of the porous silicon were obtained in the range of 320-1200 nm shown in Fig. 3. The average values for the transmittance of PSi without irradiation and with gamma irradiation (50 and 100 Gy) in the visible range of 400-800 nm were  $\sim 94\%$ ,  $\sim 92\%$  and  $\sim 90.7\%$  respectively. As can be seen with increasing  $\gamma$  irradiation, the transmittance of the PSi is decreased. Reduction in the transmittance percentage is due to the most of the incident photons are absorbed into the substrate.

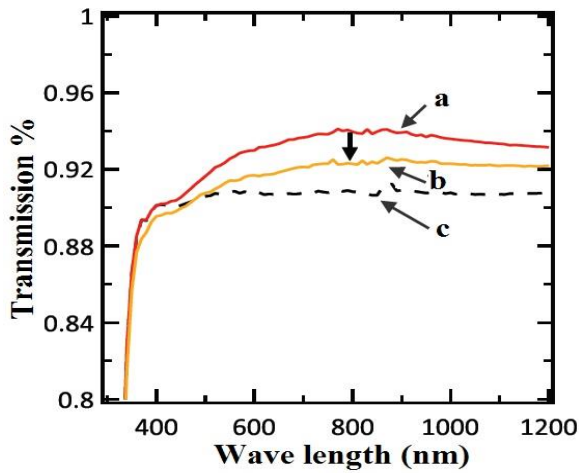


Fig. 3 – Optical transmittance spectra of PSi: without irradiation (a), irradiated at 50 Gy (b) and 100 Gy (c)

Fig. 4 shows the optical reflectance spectra as a function of the wavelength obtained for a PSi layer sample prepared by electrochemical etching. The reflection spectra of studied structures show the increasing of their optical reflectance with increasing irradiation dose. It may be caused by the absorption the most of the incident photons into the substrate [11]. The average values for the reflectance of PSi without irradiation and with gamma irradiation (50 and 100 Gy) in the visible range (400-700 nm) were  $\sim 0.82\%$ ,  $\sim 1.41\%$  and  $\sim 1.85\%$  respectively as shown in Fig. 4.

The largest ranges of the crystallites were shown in Fig. 5 which represented the PSi without irradiation and irradiated at 50 and 100 Gy respectively. All curves on the figure show PL spectra with sharp peak intensity at different wavelength which refers to a porous layer with significant silicon nanosize within the layer [12].

Due to the smaller value of the band gap energy than for photon energy of nanocrystallites, absorption led to the contribution of a large range of crystallite sizes within *n*-PSi. The PL peak intensity shows maximum valued of about 22.5, 17.5, 15.9 a.u at irradiation of 0, 50 and 100 Gy respectively. The decrease of the PL

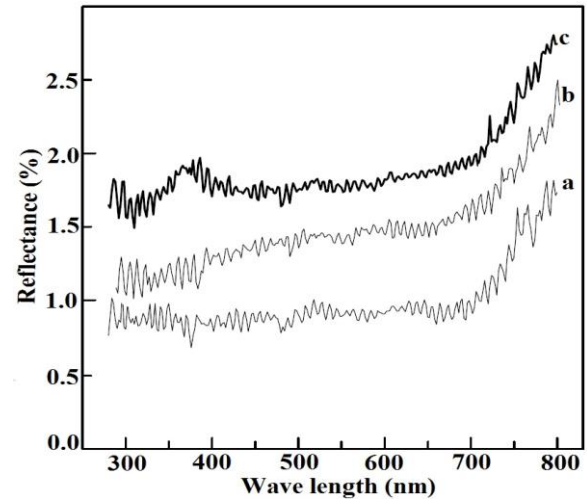


Fig. 4 – Optical reflectance spectra of PSi: without irradiation (a), irradiated at 50 Gy (b) and 100 Gy (c)

peak intensity with increasing  $\gamma$  irradiation is due to the increase of the specific surface area which increases with increasing porosity [1]. When the specific surface area increases, the density of the non-recombination centers (dangling bond) reduces to higher value, and finally the PSi material will be converted from radiative to non-radiative material [13]. From equation (1), we calculated the energy band gap of porous silicon which depends on the wavelength:

$$E_g = (h \cdot c) / \lambda, \quad (1)$$

where  $\lambda$  is the wavelength calculated from PL spectrum, nm;  $E_g$  is the energy band gap of silicon, eV;  $c$  is a speed of light in vacuum (m/s),  $h$  is Plank constant (J s).

Based on the energy gap of porous silicon in the layer, average energy band gap of nanocrystallites in the PSi layer is calculated according to the following equation (2) [14]:

$$E_g^* = E_g + 88.34/L^{1.37}, \quad (2)$$

where the porous silicon average size of nanocrystallites in the layer is  $L$  ( $\text{\AA}$ ), the energy band gap of porous silicon is represented by  $E_g^*$  (eV) and the energy band gap of bulk silicon is represented by  $E_g$  which is equal to 1.12 eV [5]. Results are outlined in Table 1.

### 3.3 Electrophysical Study

The *I-V* characteristics of PSi layer without irradiated and irradiated with  $\gamma$ -rays at 50 and 100 Gy respectively are shown in Fig. 6.

From the *I-V* measurements, we found the presented ideality factor  $n$  depends on the structure of PSi layer and is affected by irradiation.

It was increased from 1.544 to 17.563 in nanostructure layer at irradiation with  $\gamma$ -rays of 100 Gy respectively and  $n$  is calculated from Eq. (3) [15]:

$$n = q/kT \cdot dV/(d \ln(I/I_0)), \quad (3)$$

where  $dV/d \ln(I/I_0)$  is the slope of the linear region of *I-V* plots,  $q$  is the electron charge,  $k$  is the Boltzmann constant and  $T$  is a room temperature.

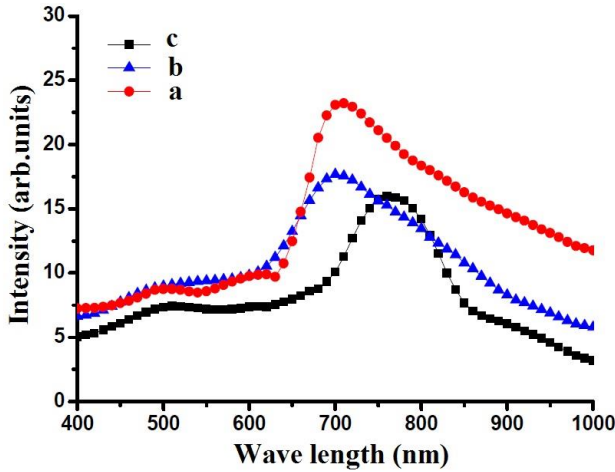


Fig. 5 – Photoluminescence (PL) peak intensity as a function of the wavelength: without irradiation (a), irradiated at 50 Gy (b) and 100 Gy (c)

Table 1 – PL spectra measurements

Sample	$\gamma$ , Gy	$\lambda$ , nm	$I_{PL}$ , a.u.	$E_g^*$ , eV	$L$ , nm
A	0	720	22.5	1.72	3.8
B	50	700	17.5	1.77	3.6
C	100	760	17.9	1.63	4.3

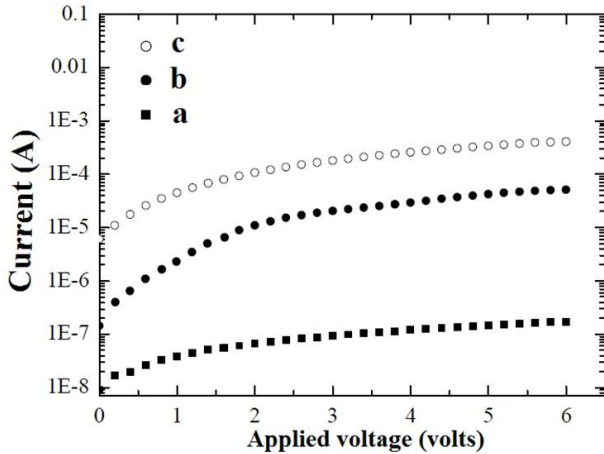


Fig. 6 – I-V curves of PSi: without irradiation (a); irradiated at 50 Gy (b) and 100 Gy (c)

We observed that the saturation current has maximum value at 100 Gy dose which increases with increasing  $\gamma$  irradiation and this corresponds to the barrier height which has small value at this point, and the decrease of the barrier height is also due to the interface between PSi layer and Si wafer which acts as a defect in the interface and leads to increase the saturation current [16].

Barrier height is given by Eq. (4) [17]:

$$\Phi_B = kT/q \ln((A/Js) \cdot T^2), \quad (4)$$

where  $A$  is the Richardson constant taken into account for  $n$ -Si [18] and equal to  $112 \text{ A}\cdot\text{cm}^{-2} \text{ K}^{-2}$ .

The measurements of electrical resistivity of the same samples were conducted using a standard four-point probe method (see Eq. (5)). It is found by measuring a direct current in the outer pair of probes and cal-

culating the voltage between the inner pair of probes which represent a distance ( $s = 1 \text{ mm}$ ) by using the relation [19] and the results are shown in Table 2.

$$\rho = 2\pi \cdot S \cdot V/I. \quad (5)$$

It is observed that the resistivity of etched layer has the high resistivity of  $10^5\text{-}10^4 \text{ }\Omega\cdot\text{cm}$  in comparison with the resistivity of the bulk substrate of  $10^{-4} \text{ }\Omega\cdot\text{cm}$  and this agrees with [20]. The resistivity of the porous silicon drastically decreases despite the  $\gamma$  irradiation dose increases. Electrical conductivity ( $\sigma$ ) increases with increasing  $\gamma$ -ray.

Fig. 7 shows the  $J$ - $V$  characteristics of the PSi layer which was prepared by electrochemical etching and irradiated with  $\gamma$ -rays at 50 and 100 Gy, respectively.

The background photocurrent (daylight current) presents a good optoelectronic response. This photoreponse is expected due to the Schottky barrier formation between the thin PSi layer and Si substrate. The daylight current shown in Fig. 7 shows an enhancement with increasing  $\gamma$  irradiation. With increasing  $\gamma$  irradiation, the size of the silicon nanocrystallites in the porous structure increases. This can lead to the formation of a PSi/ $c$ -Si heterojunction. This heterojunction may cause an increase in the total depletion layer width and hence an increase in photocurrent [21].

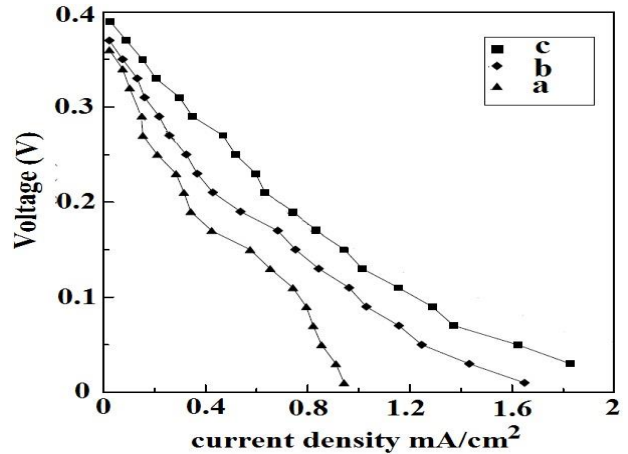


Fig. 7 – Illuminated  $J$ - $V$  plots of PSi layer: without irradiation (a), irradiated at 50 Gy (b) and 100 Gy (c)

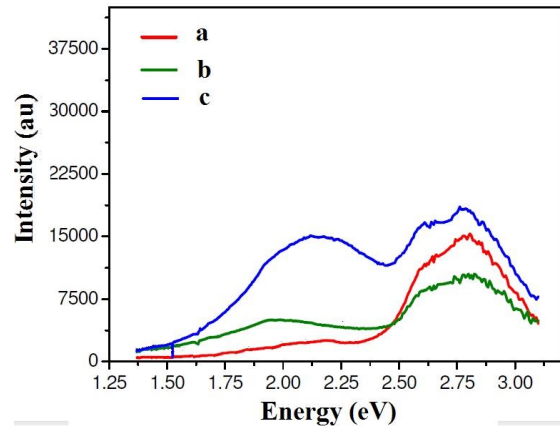


Fig. 8 – Photocurrent spectra of PSi: without irradiation (a), irradiated at 50 Gy (b) and 100 Gy (c)

**Table 2** – Electrophysical characteristics of deposited PSi films

Sample	$\gamma$ -irradiation, Gy	Voltage, V	Current, A	Resistivity $\rho$ , Ohm-cm	Conductivity $\sigma$ , Ohm-m <sup>-1</sup>	Barrier height $\Phi_B$ , eV	Ideality factor $n$ , a.u.
A	0	1	$4.0 \times 10^{-8}$	$1.57 \times 10^5$	$0.639 \times 10^{-5}$	0.855	1.544
		2	$7.0 \times 10^{-8}$	$1.79 \times 10^5$	$0.558 \times 10^{-5}$	0.841	3.833
		3	$1.0 \times 10^{-7}$	$18.84 \times 10^4$	$0.053 \times 10^{-4}$	0.831	5.962
		4	$1.5 \times 10^{-7}$	$16.74 \times 10^4$	$0.059 \times 10^{-4}$	0.821	5.366
		5	$1.6 \times 10^{-7}$	$19.62 \times 10^4$	$0.050 \times 10^{-4}$	0.819	9.757
		6	$2.0 \times 10^{-7}$	$18.84 \times 10^4$	$0.053 \times 10^{-4}$	0.814	12.620
B	50	1	$2.5 \times 10^{-6}$	$2.51 \times 10^3$	$0.390 \times 10^{-3}$	0.748	1.975
		2	$1.0 \times 10^{-5}$	$12.56 \times 10^2$	$0.079 \times 10^{-2}$	0.713	2.000
		3	$2.0 \times 10^{-5}$	$9.42 \times 10^2$	$0.106 \times 10^{-2}$	0.695	3.942
		4	$3.0 \times 10^{-5}$	$8.37 \times 10^2$	$0.119 \times 10^{-2}$	0.684	6.900
		5	$5.0 \times 10^{-5}$	$6.28 \times 10^2$	$0.159 \times 10^{-2}$	0.671	5.411
		6	$6.0 \times 10^{-5}$	$6.28 \times 10^2$	$0.159 \times 10^{-2}$	0.666	15.333
C	100	1	$6.0 \times 10^{-5}$	$1.04 \times 10^2$	$0.961 \times 10^{-2}$	0.666	1.677
		2	$1.0 \times 10^{-4}$	$12.56 \times 10^1$	$0.079 \times 10^{-1}$	0.653	5.520
		3	$2.0 \times 10^{-4}$	$9.42 \times 10^1$	$0.106 \times 10^{-1}$	0.635	7.576
		4	$3.0 \times 10^{-4}$	$8.37 \times 10^1$	$0.119 \times 10^{-1}$	0.625	9.660
		5	$4.0 \times 10^{-4}$	$7.85 \times 10^1$	$0.127 \times 10^{-1}$	0.617	13.324
		6	$5.0 \times 10^{-4}$	$7.53 \times 10^1$	$0.136 \times 10^{-1}$	0.612	17.563

Fig. 8 shows the photocurrent spectrum in the range of 1.25-3.00 eV.

Curves a and b in Fig. 8 represent one peak at energy of 2.8 eV but on curve c there are two peaks at 2.125 and 2.77 eV which lie in the visible region.

#### 4. CONCLUSIONS

This research work was devoted to the study of physical and electrical properties of porous silicon layers deposited by electrochemical etching and to the observation of the influence of  $\gamma$ -irradiation on layers characterization. PSi was synthesized by using Si wafer of  $n$ -type (111), which was rinsed by using ethanol and acetone to remove oil and dirt. SEM and cross-sectional SEM studies have been used to investigate the surface morphology and porosity of prepared samples. The growth in pore width can be attributed to an increase in the hole number on the Si surface with increasing  $\gamma$  irradiation dose. The formation of pores in the  $\langle 111 \rangle$  orientation creates side branches from the main pore. The pore growth feature persisted upon increasing  $\gamma$  irradiation to 50 Gy. As  $\gamma$  irradiation was further increased to 100 Gy, the walls were smoothed and the pores were enlarged, a behavior became more obvious at 100 Gy.

Optical properties of obtained samples were studied using the transmittance and reflectance spectra of as-deposited and irradiated samples. The average values for the transmittance of PSi without irradiation and irradiated with gamma rays (50 and 100 Gy) in the visible range of 400-800 nm were  $\sim 94\%$ ,  $\sim 92\%$  and  $\sim 90.7\%$  respectively. As can be seen, with increasing  $\gamma$

irradiation, the transmittance of the PSi decreases. Reduction in the transmittance percentage is due to the fact that most of the incident photons are absorbed into the substrate. The reflectance of PSi shows the largest reflectance with increasing irradiation. The average values for the reflectance of PSi without irradiation and irradiated with gamma rays (50 and 100 Gy) in the visible range 400-700 nm were  $\sim 0.82\%$ ,  $\sim 1.41\%$  and  $\sim 1.85\%$  respectively. This effect allows concluding the possibility of using these layers in optoelectronics industry.

Photoluminescence study has been used to estimate the band gap energies of samples. All curves in the PL spectra had a sharp peak intensity at different wavelengths which refers to a porous layer with silicon nanosize origin within the layer.

Electrophysical properties of deposited PSi layers have been studied by analyzing the  $I$ - $V$  curves of as-deposited and irradiated layers. There were measured the resistivity, conductivity, barrier height and ideality factor values. There was observed that saturation current has maximum value at 100 Gy dose and increases with increasing  $\gamma$  irradiation, and this corresponds to the barrier height with small value at this point and the decrease of the barrier height is also due to the interface between PSi layer and Si wafer which acts as a defect in the interface and lead to increase the saturation current.

The background photocurrent (daylight current) presents a good optoelectronic response. This photoreponse is expected due to the Schottky barrier formation between the thin PSi layer and Si substrate.

#### REFERENCES

1. A.K. Fedotov, S.L. Prischepa, I.A. Svito, S.V. Redko, A. Saad, A.V. Mazanik, A.L. Dolgiy, V.V. Fedotova, P. Zukowski, T.N. Koltunowicz, *J. Alloy Compd.* **657**, 21 (2016).
2. N. Naderi, M.R. Hashim, *Appl. Surf. Sci.* **258**, 6436 (2012).
3. N. Naderi, M.R. Hashim, T.S.T. Amran, *Superlattice Microst.* **51**, 626 (2012).
4. Y.Y. Xu, X.J. Li, J.T. He, X. Hu, H.Y. Wang, *Sensor Actuat. B-Chem.* **105** 219 (2005).
5. N. Naderi, M.R. Hashim, *Mater. Lett.* **88**, 65 (2012).
6. N. Naderi, M.R. Hashim, *Mater. Sci. Forum* **717-720**, 1283 (2012).
7. S.E. Lewis, J.R. De Boer, J.L. Gole, P.J. Hesketh, *Sensor Actuat. B-Chem.* **110**, 54 (2005).
8. M.A. Alwan, *Eng. Tech. J.* **31** No 3 992 (2013).
9. V. Lehmann, R. Steng, I.A. Luigart, *Mater. Sci. Eng. B* **69-70**, 11 (2000).

10. Y. Suriani, M. Abu Bakar, J. Ismail, H.H. Noor, I. Kamarulazizi, *J. Phys. Sci.* **23** No 2, 17 (2012).
11. M.N. Uday, *Eng. Techn. J.* **29** No 15, 3185 (2011).
12. F. Zhou, Y.M. Huang, *Appl. Surf. Sci.* **253**, 2690 (2007).
13. N. Bacci, A. Diligenti, G. Barillaro, *J. Appl. Phys.* **110** No 3, 036106 (2011).
14. A.M. Alwan, N.Z. Abdulzahra, N.M. Ahmed, N.H.A. Halim, *Int. J. Nanoelectron. Mater.* **2**, 157 (2009).
15. W. Fukushima, H. Harada, Y. Miyamura, M. Imai, S. Nakano, K. Kakimoto, *J. Cryst. Growth* **486**, 45 (2018).
16. B. Wu, N. Stoddard, R. Ma, R. Clark, *J. Cryst. Growth* **310**, 2178 (2008).
17. S.M. Sze, K.Ng. Kwok, *Physics of Semiconductor Devices* (New York: John Wiley & Sons: 2006).
18. S. Stolyarova, E. Baskin, Y. Nemirovsky, *J. Cryst. Growth* **360**, 131 (2012).
19. E.P. Domashevskaya, V.A. Terekhov, S.Y. Turishchev, D.A. Khoviv, E.V. Parinova, V.A. Skryshevskii, I.V. Garil'chenko, *Rus. J. Gen. Chem.* **80** No 6, 1128 (2010).
20. A.M. Ahmed, M.A. Alwan, *Eng. Technol. J.* **25** No 3, 467 (2007).
21. M.N. Uday, *Eng. Techn. J.* **25** No 5, 696 (2007).

## Оптичні та електричні властивості пористого кремнію *n*-типу, отриманого методом електрохімічного травлення та дослідження впливу на нього $\gamma$ -випромінювання

A.A. Sulaiman<sup>1</sup>, A.A.K. Muhammed<sup>2</sup>, M.M. Іващенко<sup>3</sup>

<sup>1</sup> *Department of Physics, College of Science, University of Mosul, Mosul, Iraq*

<sup>2</sup> *Сумський державний університет, вул. Римського-Корсакова, 2, Суми 40007, Україна*

<sup>3</sup> *Конотопський інститут Сумського державного університету, пр. Миру, 24, Конотоп 41615, Україна*

Шари пористого кремнію були отримані методом електрохімічного травлення. Нами було проведено дослідження фізичних та структурних властивостей шарів. Растрова електронна мікроскопія (РЕМ) та фрактографія були використані для дослідження впливу гамма-випромінювання на поруватість зразків в залежності від ступеня опромінення. Ріст поруватості у проекції ширини може бути пояснений збільшенням кількості дірок на поверхні шару кремнію при збільшенні дози опромінення. Фрактограми шарів вказують на ріст кристалітів перпендикулярно підкладці з орієнтацією росту  $\langle 111 \rangle$ . Дослідження спектрів пропускання та відбивання показало, що при збільшенні дози опромінення від 0 до 100 Гр значення пропускання зразка зменшувалося, а відбивання, відповідно, збільшувало своє значення. Дослідження спектрів фотолюмінесценції шарів вказало на те, що утворення суцільних шарів кремнію призводить до зменшення інтенсивності піків фотолюмінесценції при збільшенні інтенсивності гама-випромінювання, що пов'язане зі збільшенням площі поверхні зразка та більшим значенням забороненої зони порівняно з масивним зразком. Був проведений розрахунок таких електрофізичних параметрів, як питомі опори та провідності, висота потенційного бар'єру та фактор ідеальності. Висота потенційного бар'єру у всіх випадках мала невелике значення, що пов'язано з наявністю інтерфейсу між шаром пористого кремнію та кремнієвою підкладкою, що призводить до виникнення дефектної підструктури. При збільшенні дози опромінення з 0 до 100 Гр фактор ідеальності збільшував своє значення з 1,544 до 17,563, відповідно. Спостерігалось зменшення значення питомого опору при збільшенні значення гамма-опромінення.

**Ключові слова:** Пористий кремній, Опромінення, Електрохімічне травлення.